Effects of Steel Flexible Tracks on Forwarder Peak Load Distribution: Results from a Prototype Load Test Platform

Eric R. Labelle and Dirk Jaeger

Abstract

Steel flexible tracks (SFT) are regularly installed on bogie axles of forwarders to improve traction and extend trafficability by increasing the contact area between machines and operating surface. The study quantified dynamic peak loads exerted by a forwarder driving either on wheels or using additional SFT on its rear bogie axle. To examine load distribution of a full-scale forwarder, a load test platform was designed and constructed. Three scenarios were tested with the forwarder unloaded and loaded to quantify load distribution between wheels driven directly over the steel load test platform (Scenario 1) and SFT when either driven directly over the steel load test platform (Scenario 2) or when driven over a 20 cm layer of sand placed over the platform (Scenario 3). The platform proved to be an appropriate measuring device for full-scale tests. Results indicate that, when operated on the sand layer, SFT (installed on the forwarder's rear unloaded axle) decreased dynamic peak loads by about 30% compared to wheels. The use of SFT on bogie axles of forest machines is recommended to lower soil disturbances, especially through a reduction of peak loads often responsible for negatively altering soil physical properties.

Keywords: dynamic loads, pressure distribution, off-road traffic, forest machines, forest soils, bogie-axles, wheel loads

1. Introduction

The use of forest machines with high axle load in forest stands under off-road conditions bears the risk of negatively impacting future stand productivity and quality. These concerns have been reported for decades (Froehlich et al. 1986, Brais 2001, Murphy et al. 2004, Bygden and Wästerlund 2007). Mechanized forest operations have increased in frequency over the past half century to a level where currently most forest operations in North America and Scandinavia are fully mechanized and require the use of harvesting and extraction machines directly on soils in forest stands. In these operations, machines such as single-grip harvesters and forwarders are driven directly on machine operating trails, which are cleared openings in the stand, to permit transportation of raw forest products from the felling site to a roadside landing area. A single-grip harvester fells, delimbs, and bucks (task of cutting a stem into logs of varying lengths) trees directly in the forest stand. The harvester is then followed by a forwarder used to transport processed logs from the forest stand to a truck accessible road. The use of heavy machines, ranging between 15 to 40 metric tons (loaded), can negatively impact the operating environment by exerting high static nominal ground pressures (NGP) of 70–180 kPa directly on forest soils (Wronski and Humphreys 1994).

The performance of a vehicle is greatly influenced by the pressure it exerts on its operating surface, as sinkage and motion resistance, in particular on soft ground, are linked to ground pressure (Garber and Wong 1981). Traditionally NGP, defined as the ratio of the vehicle gross weight to the nominal ground contact area, has been widely used as a design parameter of relevance to soft ground mobility (Mellgren 1980, Garber and Wong 1981, Silversides and Sundberg 1989, Komandi 1990, Grecenko 1995). Unlike ground contact surface, which considers the total wheel surface in contact with the ground, contact area is a vertical projection of the supporting surface and is mostly used in simple models such as NGP. Contact area used

with the NGP method is based on static calculations assuming a 15% sinkage of the wheel or track wheel (rim) diameter into the soil (Partington and Ryans 2010). Because of its shortfalls, (i.e., assumed sinkage, equal contact area, equal load distribution, etc.), NGP should only be used as a guide of minimum ground pressure as it does not reflect actual pressure variation under a wheel or a track (Wong 2009). As a more comprehensive approach, the mean maximum pressure (MMP), defined as the mean value of the peak pressure magnitudes occurring under all road wheel stations (Rowland 1972), has been used to quantify and compare the performance of tracked vehicles operated on soft ground. Both formulae (Fig. 12) and sample calculations are presented in the discussion.

The combination of high ground pressure, slippage of drive wheels, and high traffic frequency on machine operating trails can cause severe impacts to soil physical properties, especially when exerted pressures exceed the soil bearing capacity. Soil compaction as a consequence of off-road vehicle travel, decreases pore quantity and soil volume (Kozlowski 1999, Poršinsky 2005). During heavy machine loadings, the disturbance of structural aggregates affects the soil thermal regime and water-air relationships as the soil is brought into anaerobic conditions (Frey et al. 2009). Most recently, the presence of anaerobic conditions is measured directly through measurement of CO_2 concentration in the soil following machine traffic (Magagnotti et al. 2012, Kleibl et al. 2014). Lower soil bearing capacity can restrict machine trafficability and increase the risk of soil disturbance (Poršinsky and Stankić 2006). Several methods (use of steel flexible tracks (SFT), use of brush mats, use of over-sized wheels, reduced tire inflation pressure, reduced payload, etc.) have been developed to increase traction and trafficability on soils at higher water contents with low bearing capacity (McMahon and Evanson 1994, McDonald and Seixas 1997, Han et al. 2006, Eliasson and Wästerlund 2007, Gerasimov and Katarov 2010, Labelle and Jaeger 2012, Edlund et al. 2013, Labelle et al. 2015, Poltorak et al. 2018). The most common technique used by forest machine owners and operators has been the installation of SFT (a.k.a. bogie tracks), which are generally constructed from semi-independent steel cross-members joined by chain links that span the entire length of a bogie axle, thus creating an oval geometry. A bogie axle is a relatively simple structure, having the advantage of decreasing the impact of surface roughness in comparison to a straight axle, which directly transmits the impact to the machine (Okamoto 1998). Unlike rigid tracks, as installed on crawler dozers, SFT do not require the use of additional rollers to support the track in between existing wheels of a bogie axle. SFT vary in width between 50 and 135 cm. By maintaining contact of the wheels even on undulating terrain, SFT serve as a mechanism for averaging and smoothing the path of the centre of gravity when the forwarder overcomes an obstacle (Potau et al. 2011). From an operational perspective, the advantages of installing SFT on forest machinery are numerous and the most beneficial aspect is their ability to distribute machine loads over a greater area, thus reducing average contact pressure (Jakobsen and Dexter 1989, Batelaan 1998, Jansson and Johansson 1998, Bygden et al. 2004, Wong 2009, Gerasimov and Katarov 2010). Increases in traction, flotation, and payload, as well as a decrease in soil compaction and rutting, are all advantages of using SFT on forest machinery (Bygden et al. 2004). Conversely, the added mass up to 4800 kg for four units (two units per bogie axle), expensive purchase price, increased fuel consumption (particularly on firm ground) damage to forest roads and the prohibition for tracked machines to travel on paved roads are the main disadvantages (Suvinen 2006).

Hornback (1998) determined that SFT increased traction compared to wheels while providing additional flexibility in terms of overcoming obstacles. Although tracks with aggressive studs or cleats welded to cross-members are usually designed for improved traction, they can also cause excessive shearing of the soil when turning, thus scalping and laterally displacing the upper soil horizon. Increased flotation due to the expanded contact area from using SFT allows greater accessibility to wet areas in harvest blocks, while the increased load distribution on a flexible surface also reduces the impact on the soil in drier conditions (Bygden and Wästerlund 2007, Olofsfors 2009). From a safety perspective, SFT increase weight distribution to the lower portion of the machine and extend the overall width, thus making the machine more stable when loading and unloading timber from the log-bunk (Olofsfors 2009). Despite the increased mass, Bygden et al. (2004) reported that SFT can reduce rut depth by up to 40% and penetration resistance by up to 10% compared to 700 mm wide wheels without SFT. Sakai et al. (2008) calculated a 20% reduction in rut depth from the use of SFT in comparison to low inflation pressure tires after 24 passes of an eight-wheel drive loaded forwarder performed directly on soil.

Under the assumption of full contact with the ground and equal loading of all track members, SFT on forest machinery have been estimated to reduce NGP by as much as 40 to 50% (Clark Forest Machine 2004, Plamondon 2006, Olofsfors 2009, John Deere 2010) compared to wheels. However, these claims are often justified by focusing entirely on the increased contact

area instead of considering load distribution characteristics. Moreover, they are performed under static conditions, which do not take into consideration maximum peak pressures exerted to an operating surface when a machine is in movement (dynamic). Considering the sagging effect of SFT (in between wheels) in relation to a fixed horizontal plane, due to the absence of support rollers and the dynamic forces, an actual measurement of dynamic peak load and ground pressure distribution would more accurately reflect the reduction achieved through the use of SFT. However, given our budget, conventional weighing systems were either too costly to purchase or could not meet the requirements (size and mass of loaded forwarders) of the study. Therefore, we designed our own prototype structure named the load test platform to measure and record dynamic loads exerted by forest machines, in particular forwarders. The aim of this study is to quantify dynamic load distribution below bogie axles with SFT and without SFT. This main research question will be addressed through the following research objectives.

1.1 Research Objectives

⇒ Design and construct a load test platform to measure and record dynamic loads of forwarders exerted on the operating surface in order to identify load distribution patterns

⇒ Quantify the impact of SFT on load distribution by comparing peak loads recorded below bogie axles with SFT to those measured below bogie axles without SFT (wheels only) when operated on a rigid surface (steel load test area) and a flexible surface (sand layer on top of the steel load test area).

2. Material and methods

2.1 Testing device – load test platform

The design of load test platform needed to address the following features: ability to test full-scale forwarders exerting high static wheel loads (up to 50 kN), sufficient width to accommodate a large forwarder (3.6 m wide) to detect load imbalances between wheels of an axle, and resistant to ruptures or tears associated with the use of branches (Labelle and Jaeger 2012). The core part of the structure was the load test area, constructed from 300 W structural quality steel (minimum yield point of 300 MPa with tensile strength of 450–620 MPa; ASTM A36 / A36M, 2004) and measuring 4.1 by 2.5 m for a total area of 10.3 m^2 (Figs. 1 and 2A). To measure and record forwarder load distribution, the load test area was equipped with 24 high capacity (450 kN) compression load cells. Each load cell was anchored to steel channels mounted to a reinforced concrete floor in order to avoid any movement and resist bending moments associated with vehicle forces due to acceleration or deceleration of the forwarder. Individual channels were spaced by 30.5 cm, each allowing for 12 load cell positions. At this spacing, channels could potentially accommodate a total of 84 load cells. However, since we were limited to 24 load cells, they were distributed on two adjacent channels over the full width of the load test area to obtain a load distribution gradient throughout the entire cross-section (Fig. 1). The surface of the load test area was constructed of 104 (12.7 mm thick) steel loading plates measuring 30.5 x 30.5 cm and each designed to support maximum loads of 50 kN. Each corner of a loading plate was supported by either a load cell or a dummy load cell, a spacer substituting load cells filling in the 60 remaining positions of the total 84 possible load cell locations. Dummy load cells were constructed from 8 mm thick steel square tubing and matched the exact height of active load cell. Due to the convex shape of the active top surface of each load cell (Fig. 1), steel top plates were designed and constructed with an indent matching the size of the active surface of the load cell, and used to expand the contact area between each loading plate and the corresponding load cells, while creating a level area of support. These 12.7 mm thick square top plates measured 10 x 10 cm and had a 4 mm deep circular indent of 6 cm radius. The flat bottom circular indents of the top plates were fitted over top of the load cells and dummy load cells with the indent facing down.

Two types of steel bracing systems, horizontal and vertical, were used to rigidify and align the channels with the frame of the load test area and the concrete floor. Remaining sections of the structure were the ramps and the in- and out-feed sections. Two ramps (1.0 m wide by 1.5 m long and 0.0 to 19.4 cm high) allowed the forwarder to approach the elevated load test area by enabling the needed vertical rise from the surrounding ground level to the 19.4 cm high in-feed section (surface slope of 13%), load test area and out-feed section (all at the same elevation). The purpose of the in- and out-feed sections (8.0 m long x 1.5 m wide) was to ensure the forwarder was completely level when approaching and departing the load test area. The load test platform was installed and all associated tests were conducted in Fredericton, New Brunswick, Canada.

2.2 Machine specifications

The machine studied was an eight-wheel (two bogie axles) Timbco TF820-D forwarder manufactured in 2001 with a tare mass of 23 500 kg and a maximum load capacity of 20 000 kg (TimberPro 2002). NGP

underneath the front wheels without SFT was 60 kPa when unloaded and 65 kPa when loaded (Makkonen 2007). When unloaded, NGP underneath the rear wheels without SFT was 35 kPa and decreased to 21 kPa when equipped with SFT. Once loaded, rear wheels exerted 64 kPa of NGP without SFT and 35 kPa with SFT. These

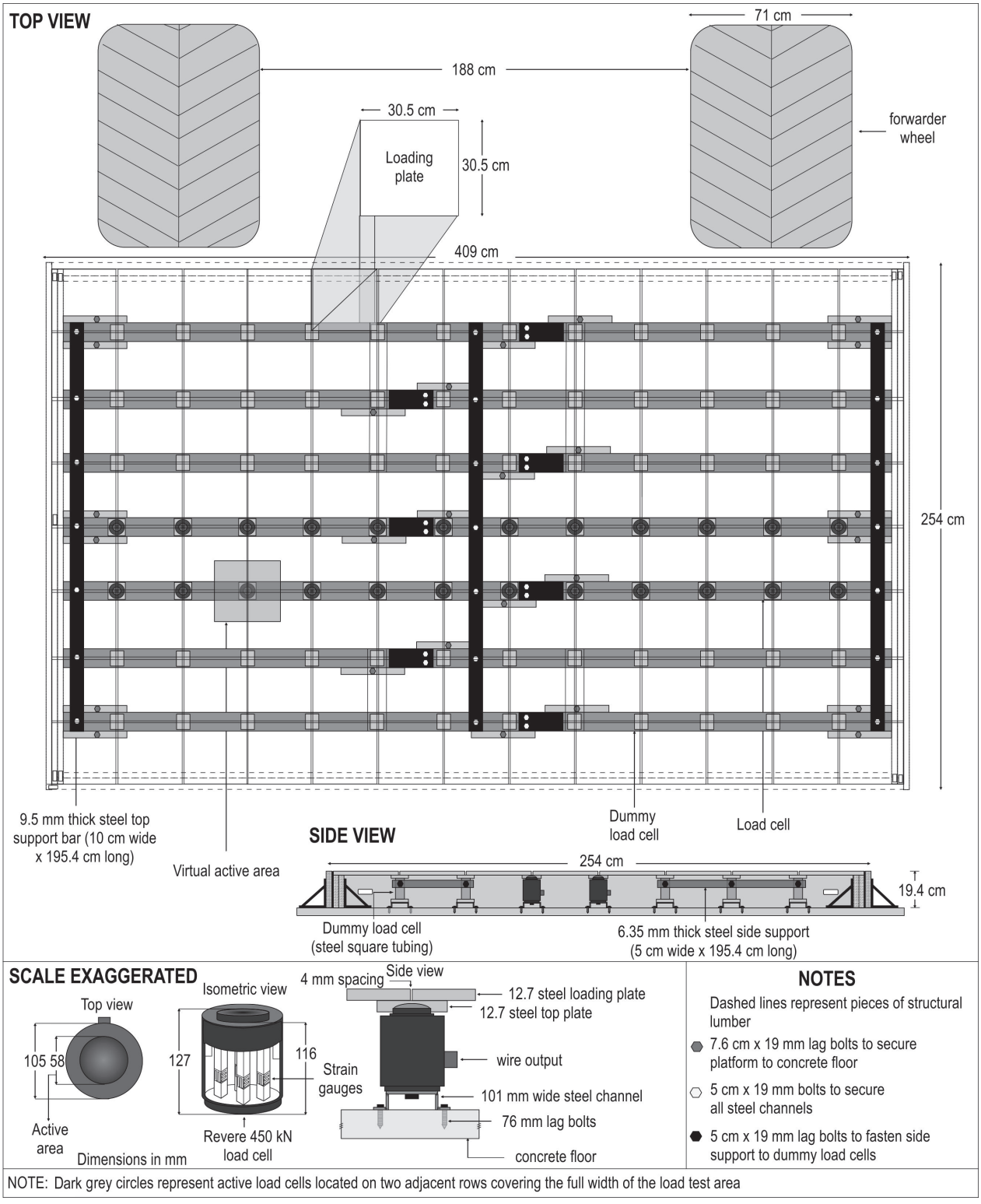

Fig. 1 Schematic of load test area

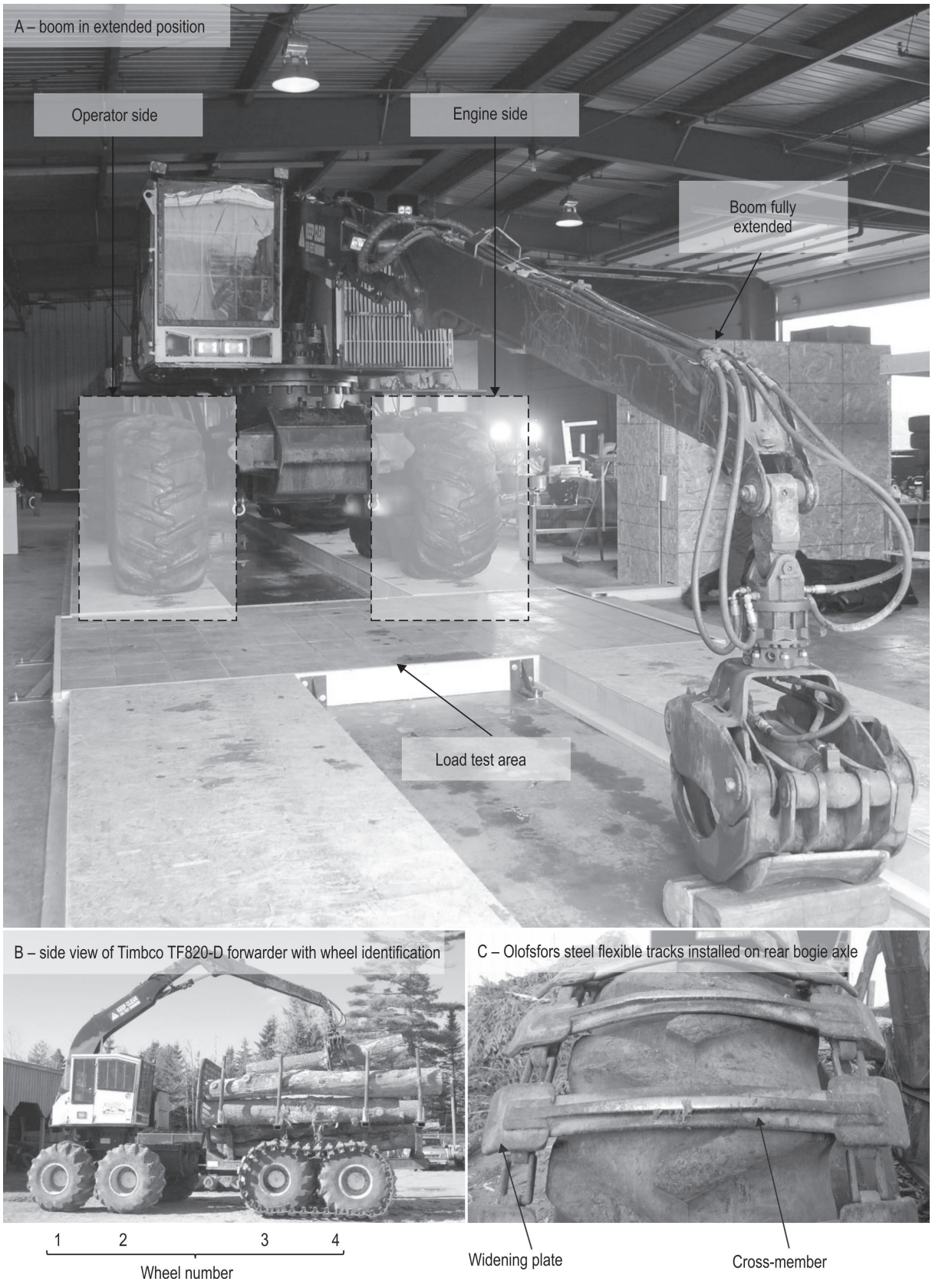

Fig. 2 View of operator and engine sides of forwarder

NGP were obtained from FPInnovations' Pascal ground pressure calculator spreadsheet (Makkonen 2007). With this spreadsheet, users can insert relevant machine parameters and directly obtain NGP based on the Mellgren (1980) formula presented in Fig. 12. Due to the high tare mass of the Timbco forwarder (23 500 kg), which is not common for forwarders used in eastern Canada, all loaded NGP mentioned above are based on the actual load (6680 kg) that was used during testing. Despite this modest load, the mass of the rear axle (13 220 kg including SFT) was determined to be only 775 kg lighter than the average rear axle mass of 8-wheel loaded forwarders (all equipped with SFT) used in eastern Canada, making findings applicable to commonly used forwarders. Testing with a 20 000 kg load would not have yielded representative results. Olofsfors steel flexible Eco-tracks weighing 1100 kg each (combined mass of 2200 kg) were installed on the rear twin-axle bogie for tests requiring the use of SFT (Fig. 2, Olofsfors 2009). Inflation pressure of all eight Firestone 28L-26 pneumatic tires remained constant at 157 kPa during testing.

2.3 Instrumentation

To acquire accurate load readings, load cells were individually calibrated using a universal 250 kN compression load frame prior to being installed on the platform. To obtain load (kN) and voltage (mV/V) relationships, direct vertical loadings were applied to each load cell by the compression load frame from 0 to 100 kN and then in reverse order from 100 to 0 kN in 10 kN increments and decrements, respectively. This range corresponded to a two-fold increase compared to the maximum loads expected at the platform. Voltage output for each 10 kN loading was recorded with a strain indicator and recorder. The similarity (<1.5% difference) between voltage outputs obtained after each respective loading for the 24 load cells suggested that a single linear calibration Eq. (1) could be applied to all load cells. Corresponding average voltage and load readings were then programmed in a 25 channel data acquisition system. Following the calibration phase, all 24 load cells were installed on the steel channels of the load test area. During dynamic and static testing, voltage measured by individual load cells was recorded at a rate of 10 readings per second and converted to load through the data acquisition system.

Eq. 1 (load cell calibration equation):

$$y = 221.82x - 0.0905 \quad (1)$$

Where:

y load in kN
x voltage in mV/V

2.4 Description of test scenarios

Three scenarios under two different testing surfaces were evaluated and dynamic loads were recorded when the forwarder was unloaded and loaded (Fig. 3). To quantify the effect of SFT on pressure distribution, tests were either performed directly over the bare surface of the steel plated load test area (rigid surface) or on top of the sand covered load test area (flexible surface). The latter was created to assess the effect of the full track/wheel contact area for distributing applied loads.

⇒ Scenario 1: Wheeled forwarder was driven unloaded and loaded (two passes each) directly over the steel load test area. Replicated three times

⇒ Scenario 2: Forwarder was driven unloaded and loaded (two passes each) directly over the steel load test area with SFT installed on the rear axle. Replicated three times

⇒ Scenario 3: Forwarder was driven unloaded and loaded (two passes each) directly over the sand covered load test area with SFT installed on the rear axle. Replicated two times.

When operated over the rigid surface, loads exerted by the forwarder were directly transferred to the steel loading plates, whereas on the flexible surface, loads were first transferred to the sand and then to the loading plates. Based on Boussinesq's (1885) equation, stress distribution within a soil profile extends both downward and outward from the point of impact (Liu and Evett 1992). This well documented stress propagation

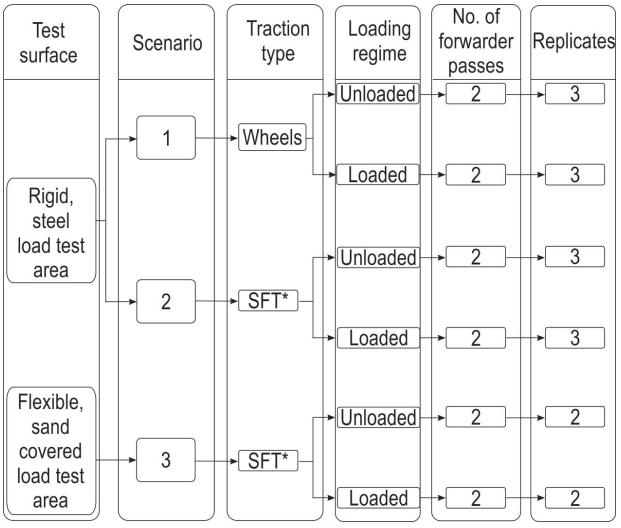

Fig. 3 Flow chart of experimental design (SFT* – steel flexible tracks)

principle, based on the theory of elasticity, is the main reason why we chose the full cross-section load cell arrangement. Because of the added distance between the operating surface and load cells (20 cm) and the stress propagation within a soil profile, arranging 12 load cells across the full width of the load test area would capture the loads laterally spread by the sand during forwarder traffic.

In each of the three scenarios, the unloaded forwarder was backed across the in-feed, the load test area, and the out-feed sections (first pass). Once the forwarder had cleared the load test area, it was driven in the opposite direction (second pass). Both machine passes were performed at a constant speed of 1.5 km h^{-1}. The traffic pattern was repeated with the forwarder loaded with 6680 kg of dry logs to ensure constant mass during the trials. Due to height restrictions at the enclosed test facility, forwarder traffic required the boom to be fully extended and directed towards the front of the machine during all test scenarios. In an effort to increase manoeuvrability over the relatively narrow in- and out-feed sections, SFT were not installed on the front bogie axle.

To allow sand to be placed on the load test platform, a wood framing system was first constructed as a measure of containment and then a 20 cm layer of mineral sand was added within the frame system. Prior to any test in Scenario 3, the sand layer was compacted in an equal spatial pattern over the entire area using a gas powered plate compactor for a period of three minutes. Once a specific test was completed (in and out movement of the forwarder), sand was thoroughly loosened with a shovel and re-compacted in the same manner and length of time as mentioned above.

2.5 Sand analyses

Following compaction by the plate compactor at the beginning of each test in Scenario 3, volumetric rings of 150 cm^3 were used to collect sand samples from two positions within the load test area (engine and operator sides). Once extracted, samples were placed in plastic bags, sealed and labelled and then taken to a laboratory for testing. Dry bulk density of the sand and gravimetric moisture content were determined by oven drying the sample at 105 °C until constant mass was reached. In addition, approx. 8 kg of sand was collected to assess general engineering properties:

⇒ particle-size distribution as determined by the mechanical sieve analysis (Bowles 1992, ASTM D 422-63 2002)

⇒ moisture and density relationship as determined by a standard Proctor test (ASTM D 698 2000).

Particle-size distribution results were used to calculate coefficients of uniformity and concavity, which provided soil classification according to the Unified Soil Classification System (ASTM D 2487 2011).

Results from the particle-size analysis indicated 80% of particles were within 0.3 and 2.0 mm in diameter with a coefficient of uniformity of 3.3 and coefficient of concavity of 1.0. The sand was classified as a poorly graded sand (SP) according to the Unified Soil Classification System. Average sand dry bulk density was calculated at 1.60 g cm^{-3} (±0.03) and average gravimetric sand moisture content was 6.3% (±0.17) throughout the test period. Using a second order polynomial curve, maximum dry density obtained from the standard Proctor test was calculated to be 1.82 g cm^{-3} at 15% optimum moisture content.

2.6 Data analysis

Depending on the time elapsed between the start and completion of a single test, over 40 000 load readings were recorded by the 24 load cells. To facilitate interpretation, only 16 load cells recording appreciable loads (>0.5 kN) were retained for all but one analysis (transect analysis; Fig. 4). Each analysis was directed at eight loading events (four loading events driving in and four loading events driving out over the load test area) corresponding to the impact of each of the eight forwarder wheels. Single loading events were characterized by an increase in load, a peak load, and then a decrease in load as a result of one wheel of the forwarder approaching, passing over, and driving away from a respective load cell.

Different resolutions (individual load cells, half cluster, cluster, and transect) could be used for analysis depending on the context. First, results from individual load cells were used to provide the highest resolution possible at the test platform (Fig. 4A). A load (kN) recorded by an individual load cell was also related to the surface area of a loading plate (0.093 m^2) to obtain surface contact pressure (kN m^{-2} or kPa). Second, to allow for a lateral load distribution analysis, the next resolution was the half cluster, corresponding to four adjacent load cells within one transect located closest to the edge of the load test platform (Fig. 4B). A total of four half clusters were used. Third, a cluster resolution was formed by combining two half clusters or eight load cells at the outermost portion of the two transects (Fig. 4C). This resolution enabled the assessment of both lateral and longitudinal load distributions and was used for wheel load verification on both

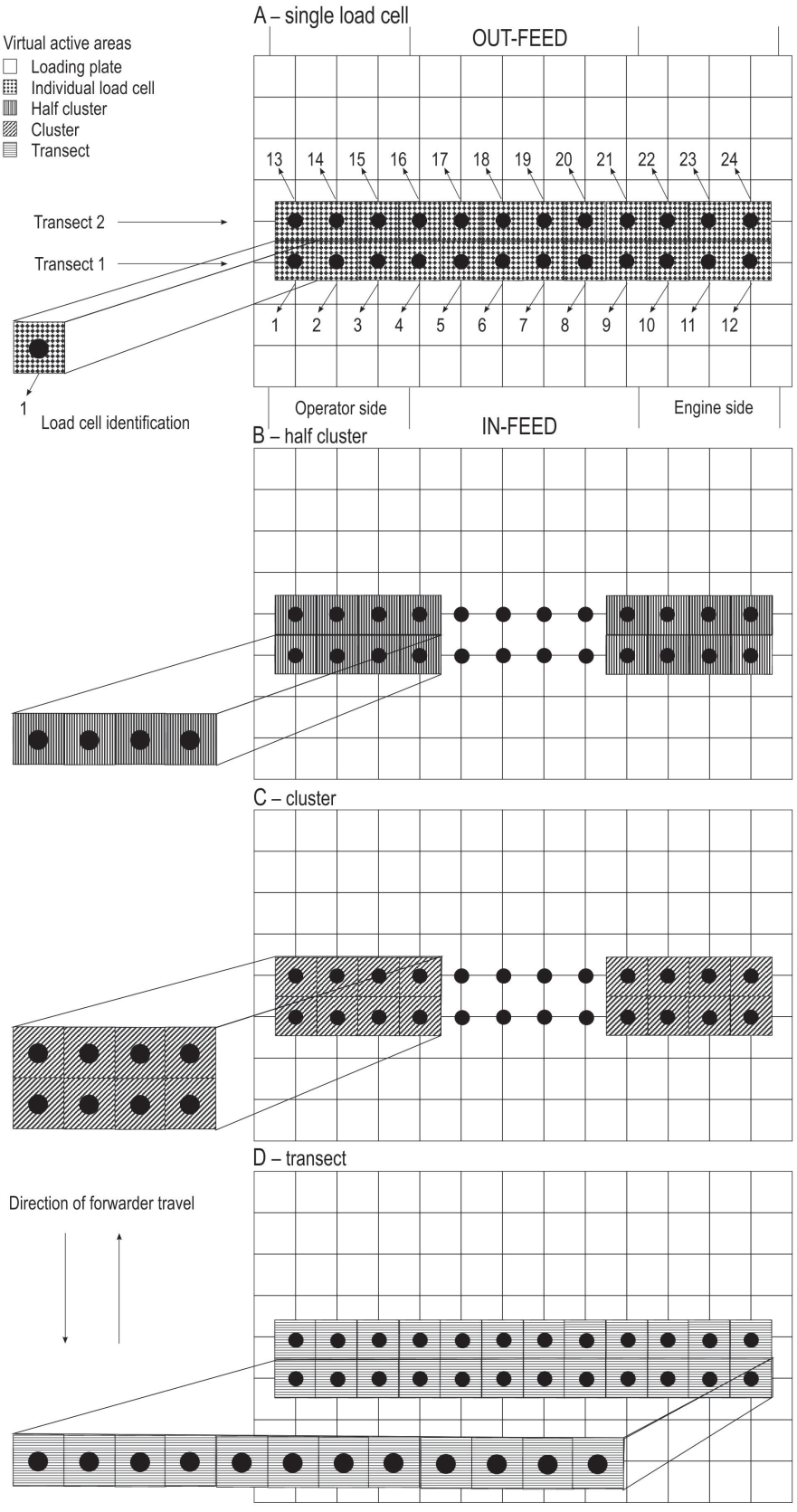

Fig. 4 Top view of load test area with active load cells identified by black circles along with different resolutions

sides (engine and operator; Fig. 2A) of the forwarder. Fourth, 12 adjacent load cells were used in the transect resolution to determine the load distributing effect over the entire cross-section of the load test area (Fig. 4D).

In addition to peak loads, the sum of peak and second highest loads obtained from adjacent load cells will be discussed. Since the impact of wheel loads on the soil is not necessarily influenced by average loading but rather by peak maximum loads exceeding the soil bearing capacity, the combined impact of the two highest peak loads per wheel was considered to avoid possible influence of machine positioning on peak load distribution to adjacent load cells. Since peak loads are dependent on the contact area, comparisons to other studies would be difficult. For this reason, peak loads (one peak per half cluster per wheel) for all replicates were converted to surface contact pressures by relating individual loads to the surface area of a single loading plate.

Static surface contact pressure thresholds for maintaining forest soil integrity vary from 35 to 80 kPa depending on soil type and soil strength (Olsen and Wästerlund 1989, Owende et al. 2002). To compensate for additional forces (vibratory, rolling, and transient) associated with dynamic testing, a dynamic surface contact pressure threshold (DSCPT) of 150 kPa for a single loading plate was assumed. The rationale behind this DSCPT is based on Rowland's (1972) mean maximum pressure formula, which uses a multiplication factor of 3.3 to the applied load to reflect the added forces associated with a moving machine. Therefore, a conservative static surface contact pressure threshold of 50 kPa was multiplied by 3 to derive the 150 kPa DSCPT. The intention was not to determine an exact threshold at which soil properties are negatively affected, but rather compare all scenarios against the same reference value.

To quantify the load diverting effect of SFT, the following steps first needed to be performed since a direct comparison of wheels vs. SFT of the rear axle on sand was not available:

Assess the impact of adding the sand layer on the loading pattern recorded by the platform.

Determine the loading impact on the front axle by adding SFT on rear axle.

Assess the load reducing effect of the sand layer by load diversion on front axle.

Apply load reduction effect on recordings of loads exerted by SFT on the rear axle when operated on sand to identify the net load diversion effect of SFT apart from the load reduction due to the sand layer.

2.6.1 Time-insensitive vs. time-sensitive methods of result analysis

Results obtained from the load cells could be analyzed and presented using two approaches referred to as time-insensitive or time-sensitive. In time-insensitive analyses, the time when individual load cells were affected by a single loading event (pass of a single wheel) was not fixed. Therefore, peak loads recorded by all impacted load cells could be obtained from different times throughout a respective loading event. With a time-sensitive approach, loads from individual load cells were recorded at a fixed/constant time during a respective loading event. When considering the impact of a forwarder on soil mechanical properties, time-insensitive results are more representative of the absolute magnitude received by the soil during a loading event. However, to accurately measure and compare wheel loads, time-sensitive results are more appropriate. Aside from transect analysis and wheel load verifications, all loads presented in this study are the result of a time-insensitive approach.

2.6.2 Wheel load verification

Portable scales were used to cross-reference the mass of each wheel from the front bogie axle (forwarder unloaded and then loaded) to the mass of wheel loads recorded at the load test platform (time-sensitive approach) when the forwarder was static. The portable scales (10 000 kg load capacity) had a 20 kg graduation and were accurate to ±50 kg when loaded between 2500 and 10 000 kg, which was the case for each wheel load measured (International Road Dynamics 2009). For proper comparison with the load test platform, the same load of 6680 kg was used for loaded measurements obtained with portable scales. During the verification of each wheel load, the boom was fully extended and located in front of the forwarder to re-create the same machine geometry used during tests performed over the load test area. Wheel loads were then compared to the static load readings at the cluster level. To assure comparable characteristics amongst measuring systems, 9 kN was added to the front axle load of the manufacturer data to account for the added mass when the boom was fully extended (portable scales and platform) in front of the forwarder instead of being placed in an upright position as was the case during manufacturer measurements.

2.6.3 Statistical analyses

To quantify the impact of SFT, data recorded at the load test platform was subjected to a one-way analysis of variance (ANOVA) with the SPSS® (SPSS 2007) and Minitab® (Minitab Inc. 2010) statistical software to determine if a statistical difference existed between the dependent variables (peak loads, second highest peak

loads, or sum of peak and second highest loads) and the independent variables (testing surface, loading regime, axle, scenario, test number, wheel number, and machine side). A significance level of 0.05 was used in all statistical tests.

3. Results

To quantify the reduction in loads by using SFT, emphasis was first directed at individual peak load cells followed by an analysis of mean peak and second highest loads. Lateral load distribution was then analyzed to quantify the SFT ability of distributing applied loads. Loads recorded at the load test area were also converted to surface contact pressures and related to a dynamic surface contact pressure threshold. A cross-reference with portable scales was also performed using a cluster resolution.

3.1 Individual peak loads

During one pass-over, each of the eight forwarder wheels caused peak loads on eight individual load

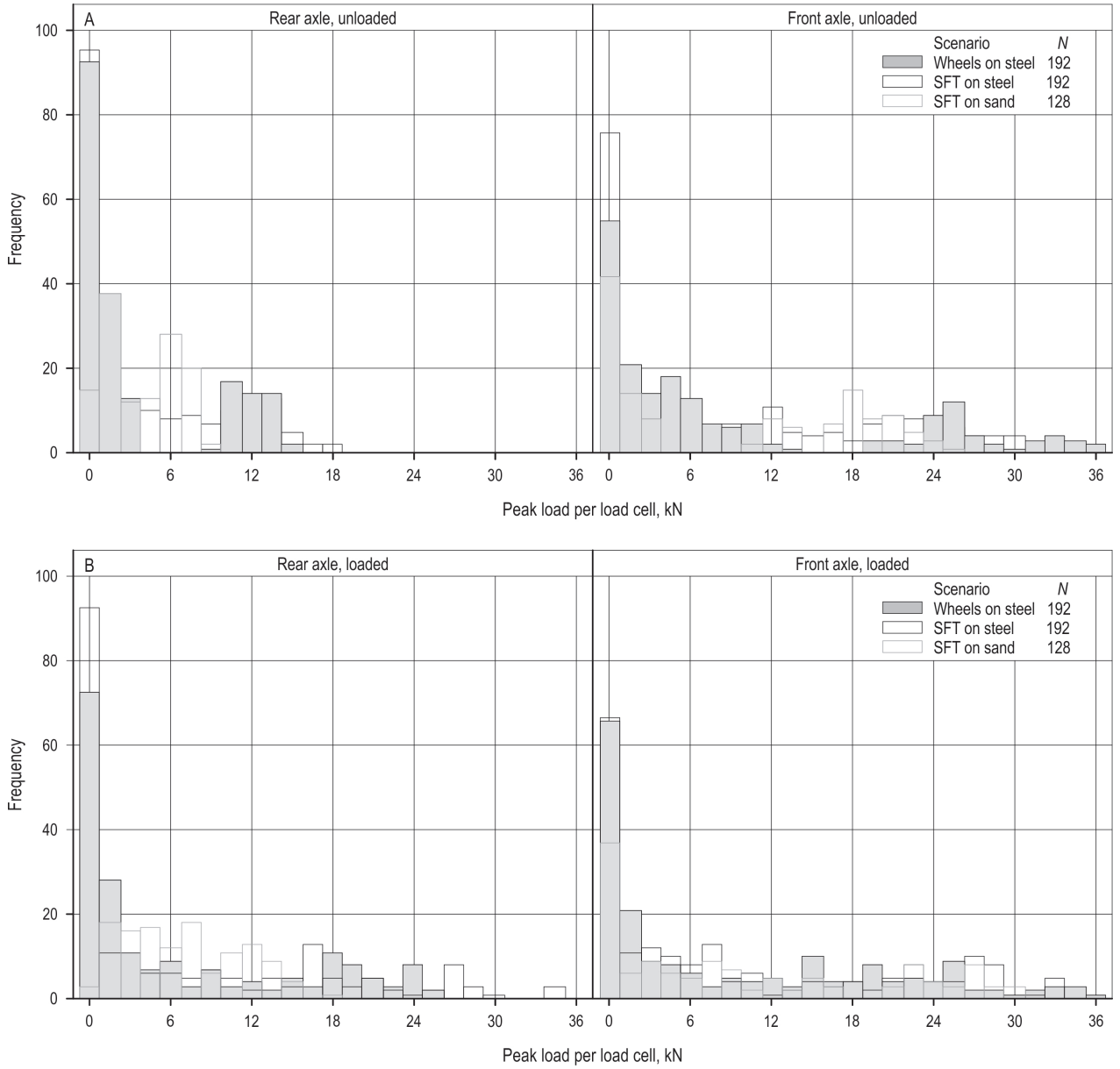

NOTE: Scenario for A) unloaded, and B) loaded forwarder (*N* = 192 (8 peak loads per machine side x 2 wheels per axle x 2 machines sides x 2 passes x 3 replicates) for Scenarios 1 and 2, while *N* = 128 for Scenario 3 since it was only replicated twice)

Fig. 5 Peak load frequency distribution per axle (single wheel)

cells (four load cells per half cluster; see Fig. 4) moving in over the test area and again moving out over the test area, which resulted in 128 peak loads. Following a one-way ANOVA showing no significant difference (p=0.893) between peak loads obtained from these two traffic patterns, all subsequent analyses will not differentiate between in and out forwarder movements. To quantify general differences between scenarios, loading regimes, and axles, peak loads were first grouped into 25 load classes of 1.5 kN to obtain frequency distributions (Fig. 5). Results were separated by axles (front and rear), thus constituting the impact of four wheel loads per axle. Figs. 5 A and B show a high frequency of peak loads in the lowest load class followed by a significant reduction of frequency as load increases to the second class. Regardless of loading regime, the highest peak load frequency corresponded to the first load class of Scenario 2.

Focusing on the rear axle, unloaded scenarios had, as expected, a higher frequency in the two lowest load classes and showed lower frequency in higher load classes than the loaded scenarios (Figs. 5A and B). When unloaded, the highest peak load class obtained in Scenario 2 was 18 kN and decreased to the 9 kN class for Scenario 3. Once loaded, peak loads recorded underneath the rear axle in Scenario 2 were up to the 34 kN class, while only reaching the 18 kN class when operated in Scenario 3. As for the front axle, results were similar between unloaded and loaded since no significant difference between frequencies of recordings in the higher load classes were detected. Variation of forwarder positioning on the load test platform between replicates may also play a key role for load distribution between adjacent load cells, thus, influencing recording frequencies within load classes, which will be addressed in the discussion section. Scenario 3 showed a reduction of the frequency of high peak loads, in particular for the rear axle.

Viewing the exerted loads from a transect perspective allowed for a better assessment of lateral load distribution for each of the scenarios. Fig. 6A to C illustrate loads exerted under a loaded condition for all four wheels per machine side driving over the platform when the sum of all 12 load cells on transect one peaked for a particular loading. In these figures, the operator side is displayed by load cells 1–4, the engine side is displayed by load cells 9–12, and load cells 5–8 have been included to show results from the entire cross-section. A change in machine positioning between replicates of the same scenario is illustrated by a different load magnitude for a respective load cell. Fig. 6A to C also demonstrate whether the load was mostly spread over one, two, or three adjacent load cells. In Scenario 1, loads of wheels 3 and 4 were mostly recorded by only one load cell, while in Scenario 2 wheel loads were spread across two load cells. Scenario 3 clearly showed lateral distribution of the wheel loads over two, three, and occasionally four load cells.

3.2 Relationship between peak and second highest loads

Positioning of the forwarder in relation to the load test area could influence the distribution and magnitude of recorded peak loads by either exerting most of the load to a single load cell or by spreading it between two adjacent load cells. Therefore, the second highest load originating from a load cell adjacent to where the peak load was recorded was expressed in percent of the peak load (Fig. 7). An equal distribution between the second highest load and peak load would represent 100% on the ordinate and having the load distributed to a single load cell would be indicated by 0%, thus not transferring any load to an adjacent load cell. Aside from the front axle in the loaded tests, an increase of the second highest load in relation to peak load was detected as scenarios increased from 1 to 3 (Fig. 7) with the highest percentage (between second highest and peak) observed in Scenario 3. When focusing on the loads of the rear axle in the unloaded regime, there was very little variation between the relative loads of the load cells and the second highest loadings. On average (all tests combined), the second highest loads amounted to 16.3, 37.4, and 78.9% for Scenarios 1, 2, and 3, respectively (Fig. 7A). This means that once the forwarder was operated over the sand covered load test area, the load cell adjacent to where the peak load was recorded would record on average almost 80% of the peak load. Aside from differences between replicates for Scenario 2, wheel loads of the front axle in the unloaded scenario showed very similar results to the loads recorded of the rear wheels in the unloaded scenario. Variation of the second highest recorded loads in percent of the peak loads was much higher between tests within a scenario when the forwarder was loaded (maximum variation of 31%) compared to when it was unloaded (maximum variation of 18%). Unlike most cases in the unloaded regime, once loaded, the second highest loads in percent of the peak loads were lowest in Scenario 3. In fact, the second highest loads in percent of the peak loads were highest for the most part with Scenario 1. Upcoming analysis will attempt to provide reasons for such high variation when the log-bunk was loaded.

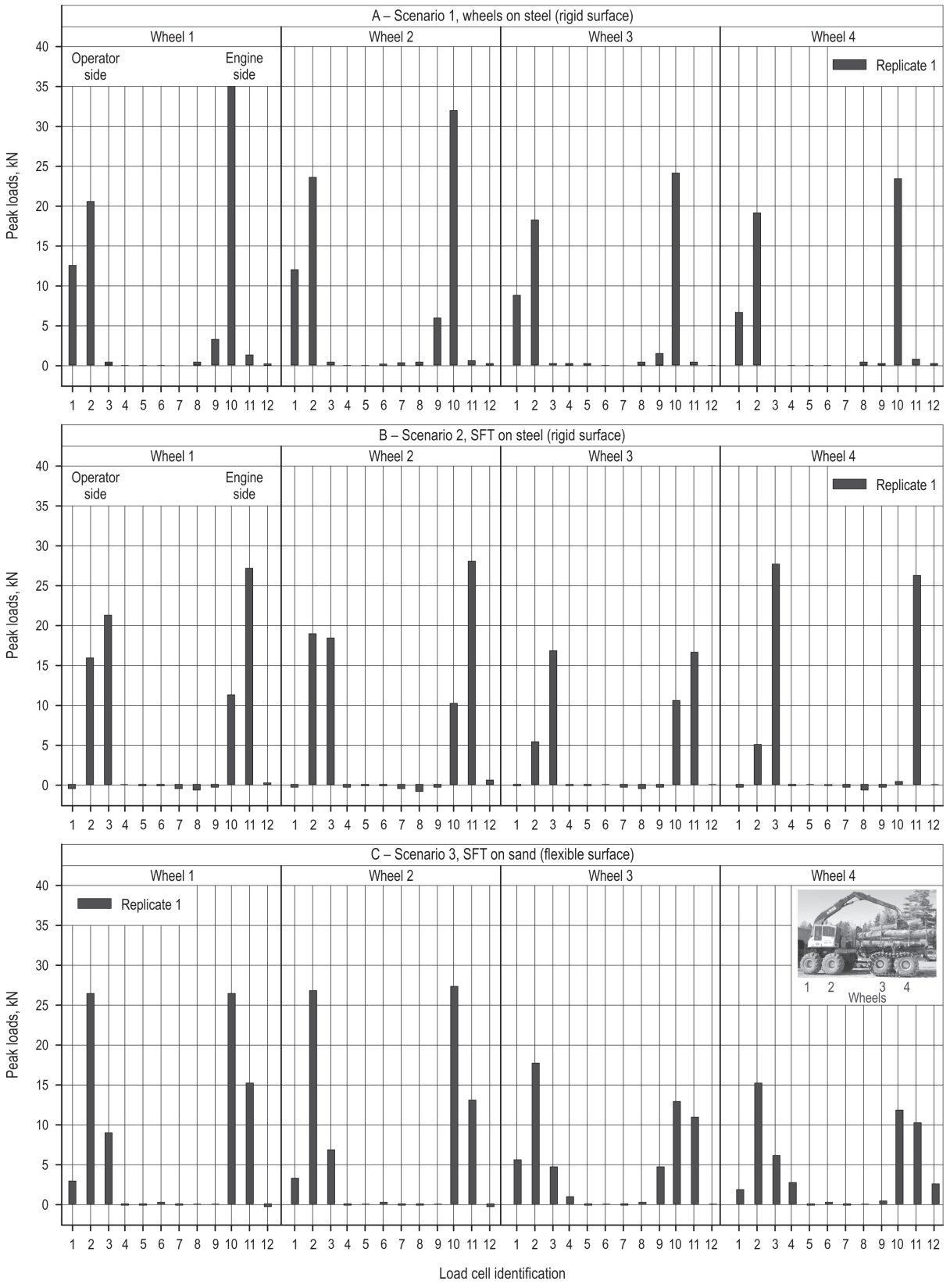

Fig. 6a Peak loads across transect one occurring during replicate 1. Each graph shows loads (when the sum of all 12 load cells on transect 1 peaked: time-sensitive) exerted by the forwarder within a scenario

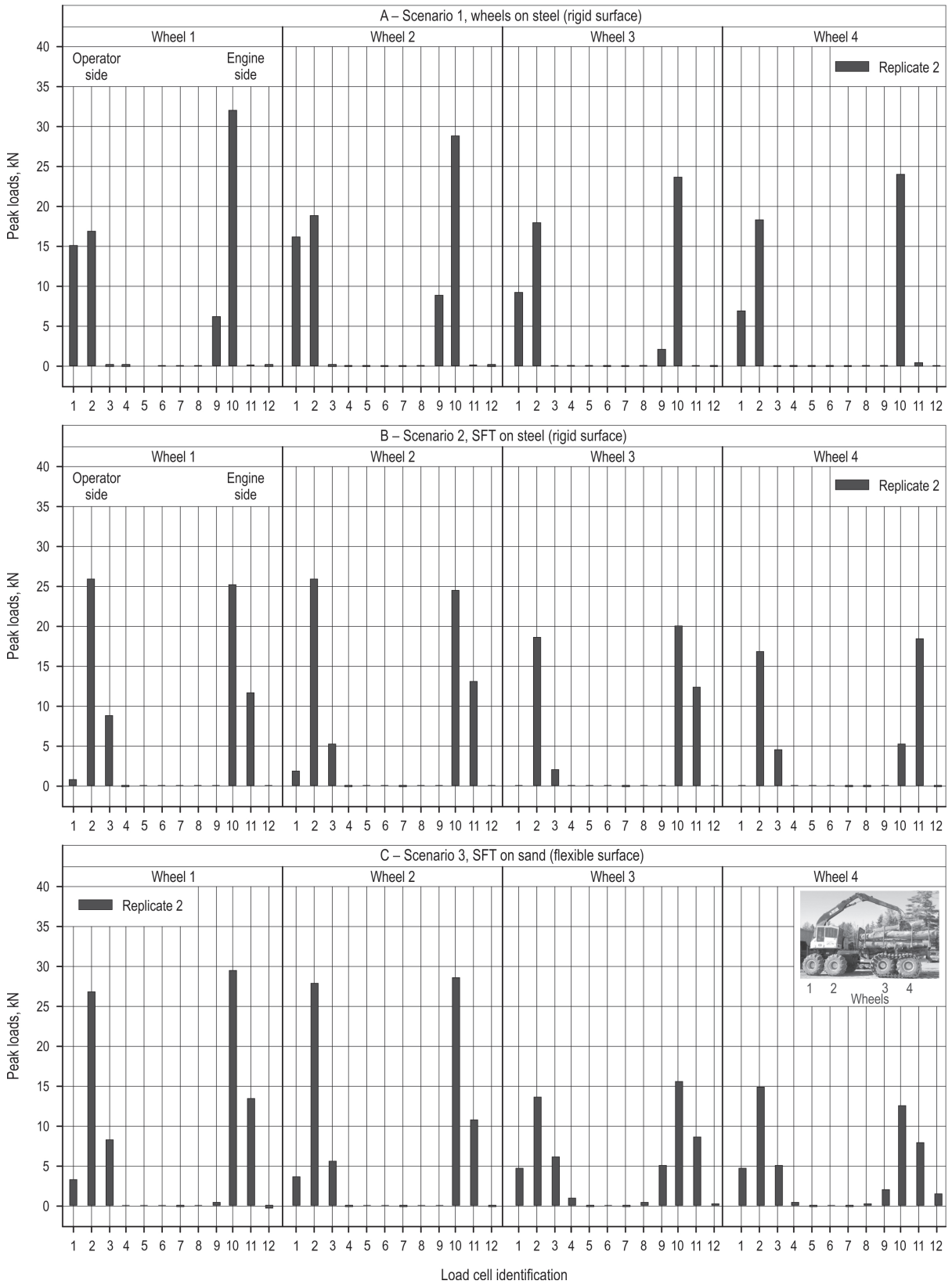

Fig. 6b Peak loads across transect one occurring during replicate 2. Each graph shows loads (when the sum of all 12 load cells on transect 1 peaked: time-sensitive) exerted by the forwarder within a scenario

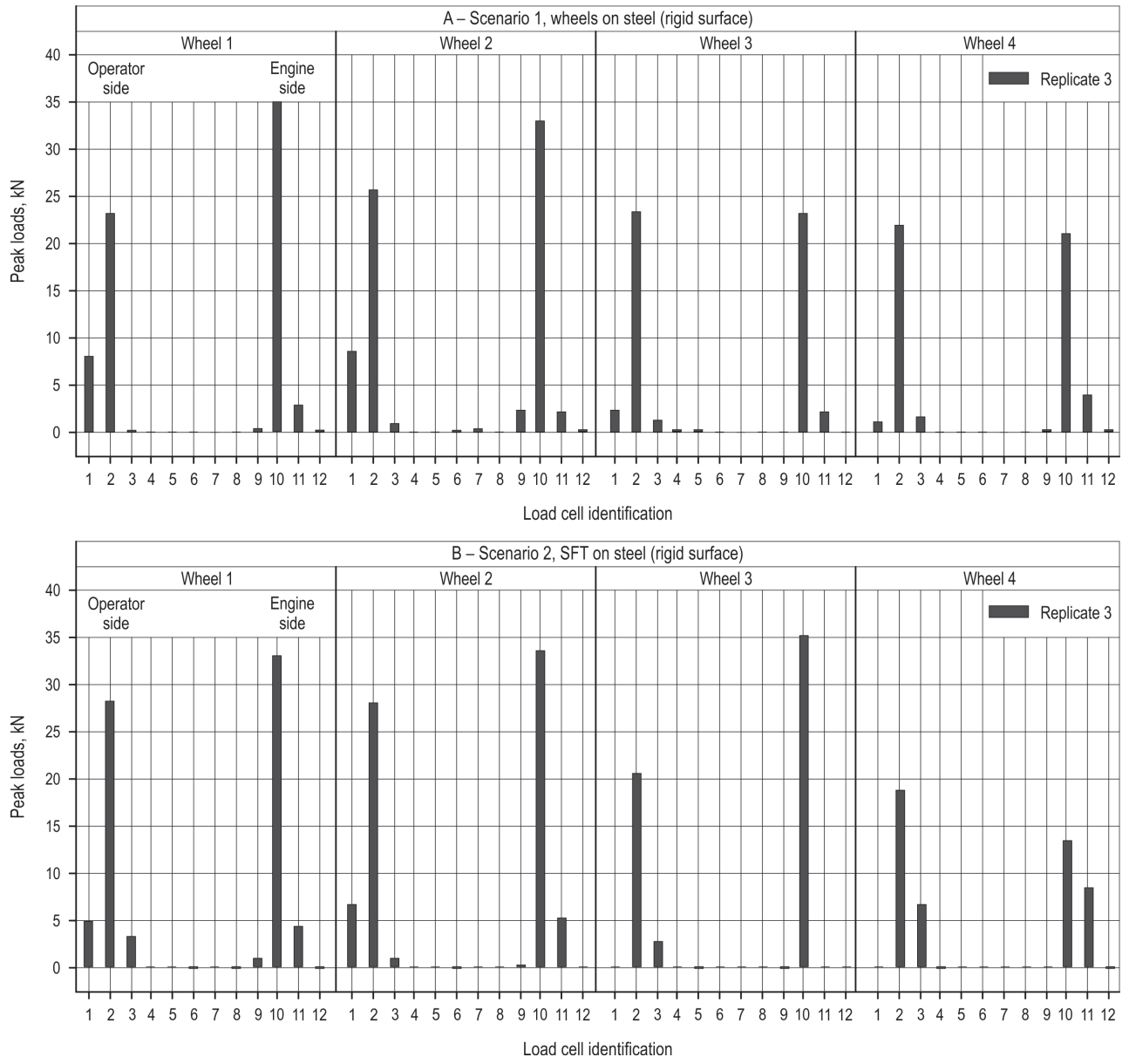

Fig. 6c Peak loads across transect one occurring during replicate 3. Each graph shows loads (when the sum of all 12 load cells on transect 1 peaked: time-sensitive) exerted by the forwarder within a scenario

3.3 Mean peak loads and second highest loads

Mean peak loads obtained by loading regimes and axles were plotted (Fig. 8). Statistically different mean peak loads (p=0.000) were recorded underneath the rear axle between Scenarios 1 and 3 when unloaded and between all three scenarios when loaded. The sand layer lowered mean peak loads exerted below the rear axle by 42% for both unloaded and loaded loading regimes compared to loads recorded below SFT on a rigid surface. Compared to wheels on the rigid surface, the addition of SFT on the rear unloaded axle increased mean peak loads by 2.2% and by 12.1% when loaded. Mean peak loads recorded underneath wheels of the front axle in the unloaded regime decreased by 11% from Scenario 1 to 2, and another 12% between Scenarios 2 and 3 with a statistical difference between each scenario (p=0.000 Scenarios 1 vs. 2, and p=0.000 Scenarios 2 vs. 3). When loaded, mean peak loads exerted below the front wheels did not show the same trend as when unloaded. In fact, no statistical difference was detected between scenarios. Regardless of axle, loading regime, or traction type, the lowest

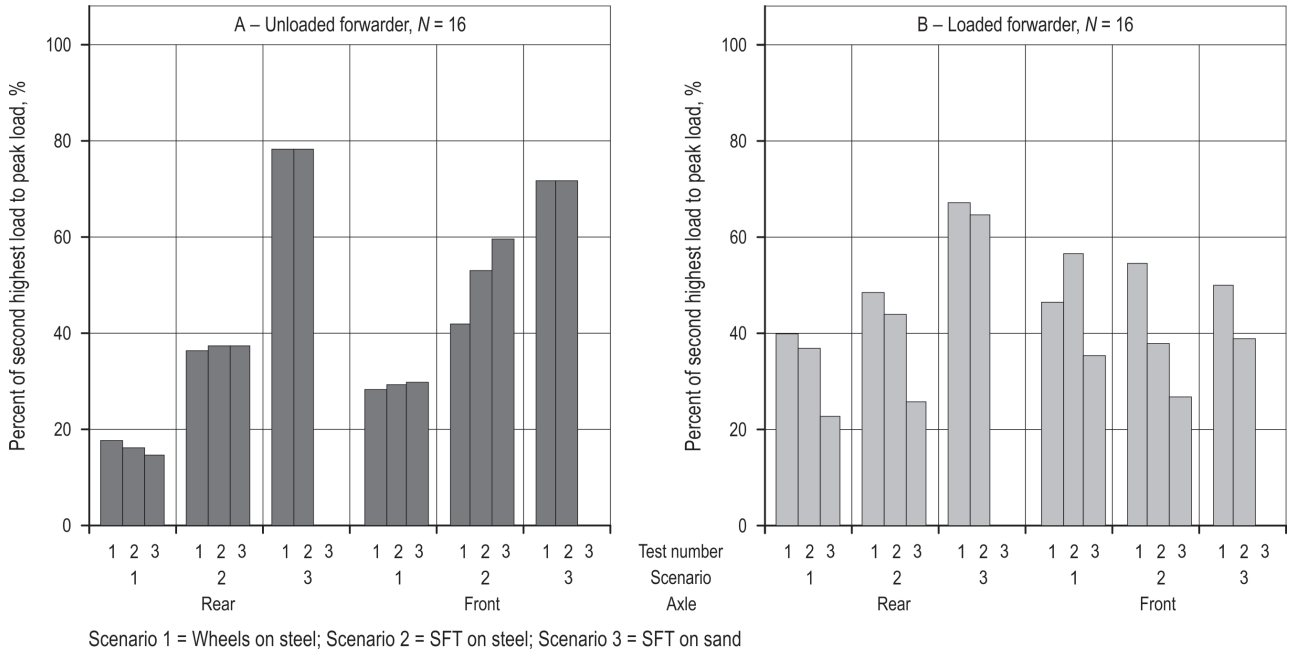

Fig. 7 Mean percent of second highest load to peak load per test number, scenario, and axle (N=16 is derived from 1 peak load per transect x 2 transects x 2 wheels per axle x 2 machine sides x 2 passes)

mean peak loads were recorded in Scenario 3 when the forwarder was operated over the flexible sand layer.

When considering the second highest loads, a clear trend of higher load distribution was detected for both Scenarios 2 and 3 when SFT were present (Fig. 9).

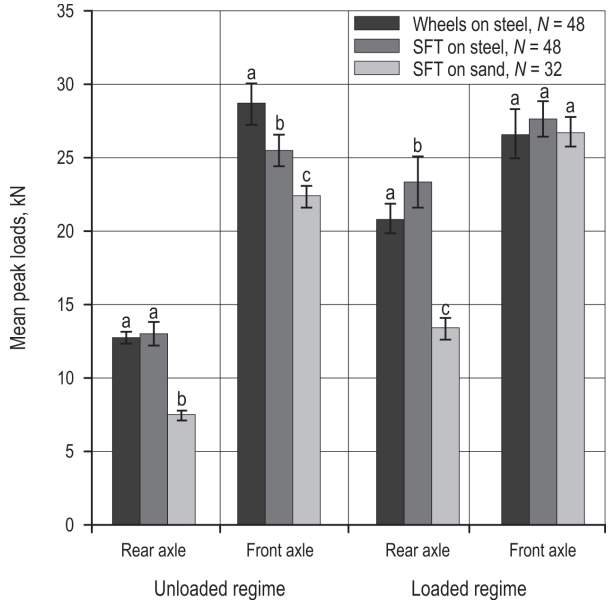

Fig. 8 Mean peak loads per axle, loading regime, and scenario (different letters indicate a statistical difference between scenarios at the 0.05 probability level; N=48 is derived from (1 peak load per transect x 2 transects x 2 wheels per axle x 2 machine sides x 2 passes x 3 replicates) for Scenarios 1 and 2, while N=32 for Scenario 3 since it was only replicated twice)

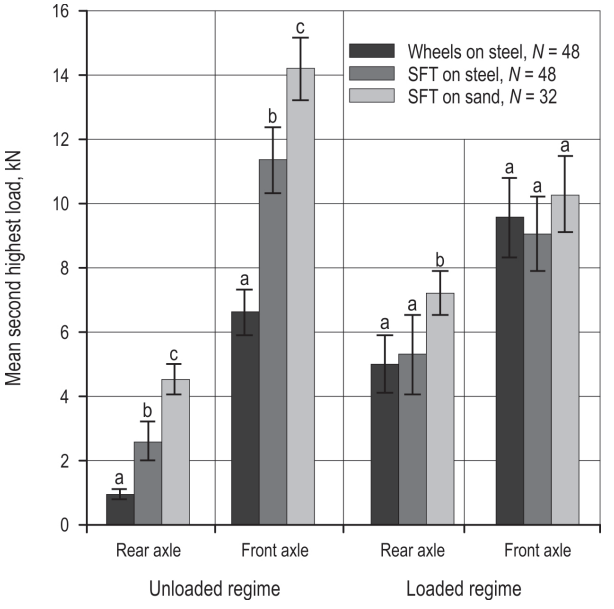

Fig. 9 Mean second highest loads per axle, loading regime, and scenario (different letters indicate a statistical difference between scenarios at the 0.05 probability level; N=48 is derived from (1 peak load per transect x 2 transects x 2 wheels per axle x 2 machine sides x 2 passes x 3 replicates) for Scenarios 1 and 2, while N=32 for Scenario 3 since it was only replicated twice)

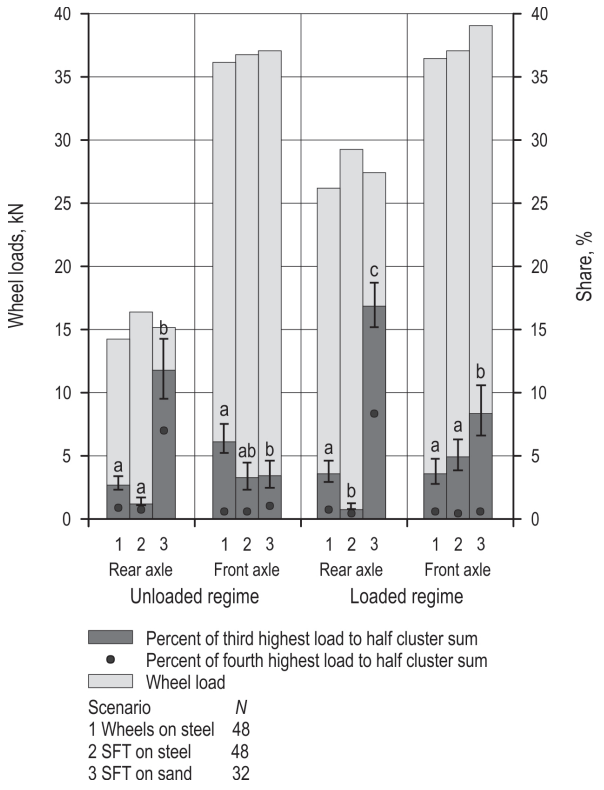

Fig. 10 Mean wheel loads obtained from the sum of four load cells wide (half cluster) per scenario, axle (single wheel), and loading regime are presented by light grey bars and relate to the left ordinate. The right ordinate represents the mean third highest load in percent of the half cluster sum (dark grey shaded bars) and the mean fourth highest load in percent of the half cluster sum (dots). Different letters indicate a statistical difference of the mean third highest load in percent of the half cluster sum between each scenario for a respective axle and loading regime at the 0.05 probability level. $N=48$ is derived from (1 peak load per transect x 2 transects x 2 wheels per axle x 2 machine sides x 2 passes x 3 replicates) for Scenarios 1 and 2, while $N=32$ for Scenario 3 since it was only replicated twice

When unloaded, statistical differences between each scenario (p=0.000 Scenario 1 vs. 2, and p=0.000 Scenario 2 vs. 3) were observed for both axles with mean second highest loads reaching 4.6 and 14.4 kN in Scenario 3 for rear and front axles, respectively. A similar trend of higher mean second highest loads was also seen for the rear axle when loaded. In this case, mean second highest loads increased by 35% between scenarios 2 and 3. Results from the front axle when the forwarder was loaded were less variable between scenarios.

3.3.1 Load distribution

To gain further insight into lateral load distribution, the third highest load was expressed in percent of the sum of a related half cluster as indicated by the right ordinate of Fig. 10. The general assumption was that an increase in contact area between the running gear and the operating surface would most likely reduce maximum peak load, while increasing the load exerted on surrounding load cells. To describe the relative magnitude of loads received by single load cells, we related them to the sum of the four load cells of the half cluster they belong to and presented them in Fig. 10 using the left ordinate. Aside from an increased wheel load associated with the addition of SFT on the rear bogie axle (on average 13.5% higher for the rear bogie compared to Scenario 1), wheel loads were quite consistent when the forwarder was operated over the steel platform. In Scenario 3, higher wheel loads of 7.7 and 5.4% were recorded for the front loaded axle compared to Senarios 1 and 2, respectively.

When unloaded, mean third highest load in percent of the half cluster sum decreased for the rear axle from 2.7 to 1.2% for Scenarios 1 and 2, respectively (Fig. 10). In Scenario 3, the third highest load from the unloaded rear axle increased to 11.8% of the half cluster sum, which was statistically different from other scenarios. Similar results were obtained once loaded, with the third highest load representing 3.6, 0.8, and 16.9% of the half cluster sum for Scenarios 1, 2, and 3, respectively, with statistical differences detected between all three scenarios.

To further assess lateral load distribution from the point of contact, the fourth highest mean load in percent of the half cluster sum, indicated by black dots, was considered and presented using the right ordinate to express the relative magnitude in percent (Fig. 10). Similar to responses from the third highest load, results from fourth highest loads in relation to half cluster sum indicated higher loads when operated over sand. Mean response of the fourth highest load was consistently below 1% of the half cluster sum until the forwarder was operated over the sand layer, where it increased to 6.7 and 8.1% for the rear unloaded and loaded axles, respectively.

3.4 Surface contact pressure

The addition of the sand layer concentrated peak surface contact pressures in a narrower range compared to the other two scenarios (Fig. 11). When unloaded, 8, 19, and 0% of peak pressures recorded underneath the rear axle exceeded the DSCPT for Scenarios 1, 2, and 3, respectively. Once loaded, 96, 96, and 19% of peak pressures recorded underneath the rear axle exceeded the DSCPT for Scenarios 1, 2, and 3, respectively. The entirety of the data set from the front axle exceeded the DSCPT. Other than concentrating

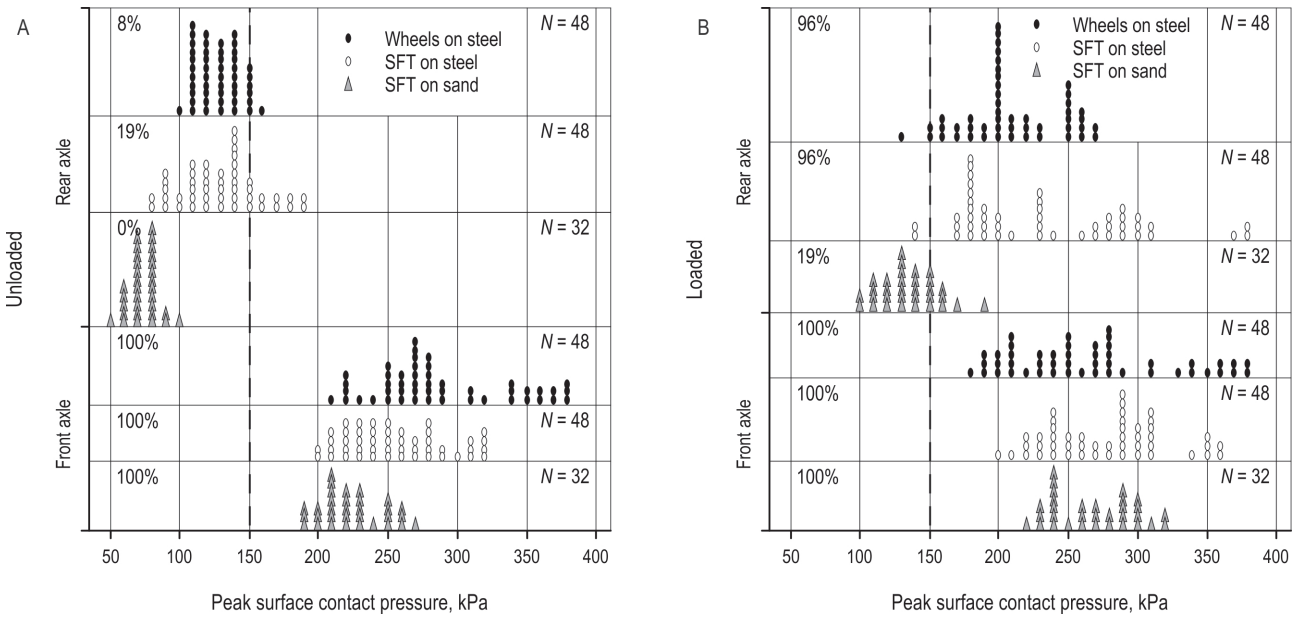

Fig. 11 Peak surface contact pressure frequency distribution per axle and scenario for A) unloaded and B) loaded loading regimes. Percentage of peak loads exceeding the dynamic surface contact pressure threshold of 150 kPa as identified with the vertical dashed line are presented near the left ordinate. *N*=48 is derived from (1 peak load per transect x 2 transects x 2 wheels per axle x 2 machine sides x 2 passes x 3 replicates) for Scenarios 1 and 2, while *N*=32 for Scenario 3 since it was only replicated twice

peak pressures to a narrower range, the addition of the sand layer did not seem to have the same effect for the wheeled front axle as it did for the tracked rear axle.

3.5 Effects of steel flexible tracks on load distribution

Mean peak loads were used to establish percent differences between each scenario for respective loading regimes and axles (Table 1). A negative percent difference indicated a reduction of Scenario 2 in relation to Scenario 1 used as comparison e.g. comparing Scenarios 1 and 2 of the front unloaded axle show a percent reduction of –11%, thus indicating 11% lower mean peak loads for Scenario 2 compared to Scenario 1. The percent differences could be influenced by the use of SFT, the addition of the sand layer, or more likely a combination of both factors. While it was essential to consider the effect of SFT on mean peak loads within a loading regime, omitting the contributing effect of the sand layer on potential mean load reduction below the sand could overestimate the effect of using SFT.

Table 1 Percent reduction from sand versus steel load test platform and from tracks versus wheels

Loading regime	Axle	Scenarios compared	Percent difference	Effect of rear tracks	Effect of sand
Unloaded	Front	Wheels on steel vs. SFT on steel (1 vs. 2)	–11.0%	11%	N/A†
		Wheels on steel vs. SFT on sand (1 vs. 3)	–22.0%	11%	11%
	Rear	Wheels on steel vs. SFT on steel (1 vs. 2)	+2.2%	2.2%	N/A
		Wheels on steel vs. SFT on sand (1 vs. 3)	–41.6%	30.6%	11%

† = not applicable

When considering the rear axle, it was rather complicated to differentiate between the effect of SFT and sand on mean peak loads. To quantify the perceived load reductions caused by sand on the loads exerted by the rear unloaded axle, the reduction incurred by the sand layer for the front axle was assumed to be the same for the rear axle. This meant that, in the unloaded scenarios, a reduction of 11% in mean peak loads was assumed to be caused by the addition of the sand layer and was, therefore, subtracted from the total percent reduction observed (Table 1). By accounting for the magnitude of mean load reduction caused by the sand layer underneath the front axle (11%), and observing the total percent reduction caused by the sand and SFT on the rear axle (41.6%), a total reduction of

30.6% was calculated and attributed to the use of SFT on the rear unloaded axle.

Due to higher variation in machine positioning in relation to the load test area once the forwarder was loaded (caused by limited visibility) and its inherent effect on peak load distribution as presented in Fig. 6A to C, extending the analysis to the loaded regime would not be meaningful.

3.6 Wheel load verification

As a cross-reference, individual wheel loads were compared between measurements obtained with the load test platform to those from portable scales and manufacturer data (Table 2). Since the addition of SFT on the rear axle complicated the use of portable scales by increasing the contact area now linking both wheels, only wheel loads obtained from the front axle are presented. Compared to manufacturer data, front axle loads were overestimated by 2.5% and 8.8% for portable scales and results from the platform, respectively.

Table 2 Front unloaded axle load comparisons between Timberpro (manufacturer of Timbco TF-820D forwarder), portable scales, and static time-sensitive results from the load test platform (cluster resolution)

Measuring system	Axle load kN	Boom position	% diff. to Timberpro with boom extended	% diff. to portable scales
Timberpro	151 [160] †	Upright	0	–2.4
DOT scales	164	Extended	+2.5	0
Platform	174	Extended	+8.8	+6.1

† The front axle of Timbco forwarder was 9 kN heavier when the boom was fully extended and facing the front of the forwarder compared to when it was in an upright position. Since all forwarder movements on the load test platform required the boom to be fully extended, this load of 9 kN was added to the mass of the front axle obtained from Timberpro

4. Discussion

4.1 Ground pressure calculations

To facilitate the understanding of the NGP concept, sample calculations for a pneumatic tire and SFT are presented in Fig. 12 (Mellgren 1980). Considering actual dimensions of the forwarder and wheels used in this study, the following parameters would apply: b=0.71 m, B=1.05 m, R=0.82 m, L=1.70 m, h=0.5 m, and δ=0.078 m. Assuming identical single wheel loads (G_w) of 50 kN and SFT weight (G_t) of 10.8 kN (1100 kg for each SFT), NGP underneath the front wheel would equal 86 kPa and 39 kPa underneath the rear bogie axle equipped with SFT, translating to a 54.7% reduction of NGP with the use of SFT.

Based on Rowland (1972) MMP formula and using the same parameters as used in the NGP example, a MMP of 179.4 kPa underneath the front wheel was calculated, which corresponds to a 108.6% increase compared to the standard NGP method (Fig. 12). Calculating MMP underneath the rear bogie axle equipped with SFT was not possible since no formula has been adapted for such flexible tracks. Applying a rigid track MMP formula to flexible tracks would not yield representative results (MMP estimates would be too low) due to the different dynamics and geometry of the running gear, in particular the absence of support rollers.

Peak loads and surface contact pressures discussed in this article were recorded with the forwarder in motion and are therefore dynamic measurements. Maximum peak surface contact pressures (related to single loading plates) recorded underneath the single wheels from the rear axle equipped with SFT were as high as 300 kPa when operated directly over the steel load test area, equalling approx. a seven-fold increase compared to NGP calculated for the same axle (39 kPa). According to Wong (2009), MMP exerted by a tracked vehicle can be as much as 14 times higher than the NGP. Maximum pressures are particularly crucial when considering the impact of a machine on soil physical properties. Once a vehicle is in motion and operated on harder surfaces, actual peak pressures, localized on the side of tire lugs will cause the most severe damage to the soil. Minimizing the magnitude of these maximum pressures is an essential component to maintain soil integrity.

4.2 Effect of different running gears on load distribution

The use of SFT on the rear bogie axle caused the highest mean peak loads compared to when the forwarder was operated without SFT directly on the steel load test area. This trend is most likely caused by three factors:

⇒ the geometry of SFT is such that only track cross-members spaced 25 cm apart are distributing loads to the steel platform. The location at which a cross-member came into contact with a loading plate varied with the forwarder movements and potentially resulted in identical wheel loads being recorded differently by the load cells

⇒ cross-members have a u-shaped geometry that tends to concentrate loads in the centre of the track in relation to its width (Fig. 2C)

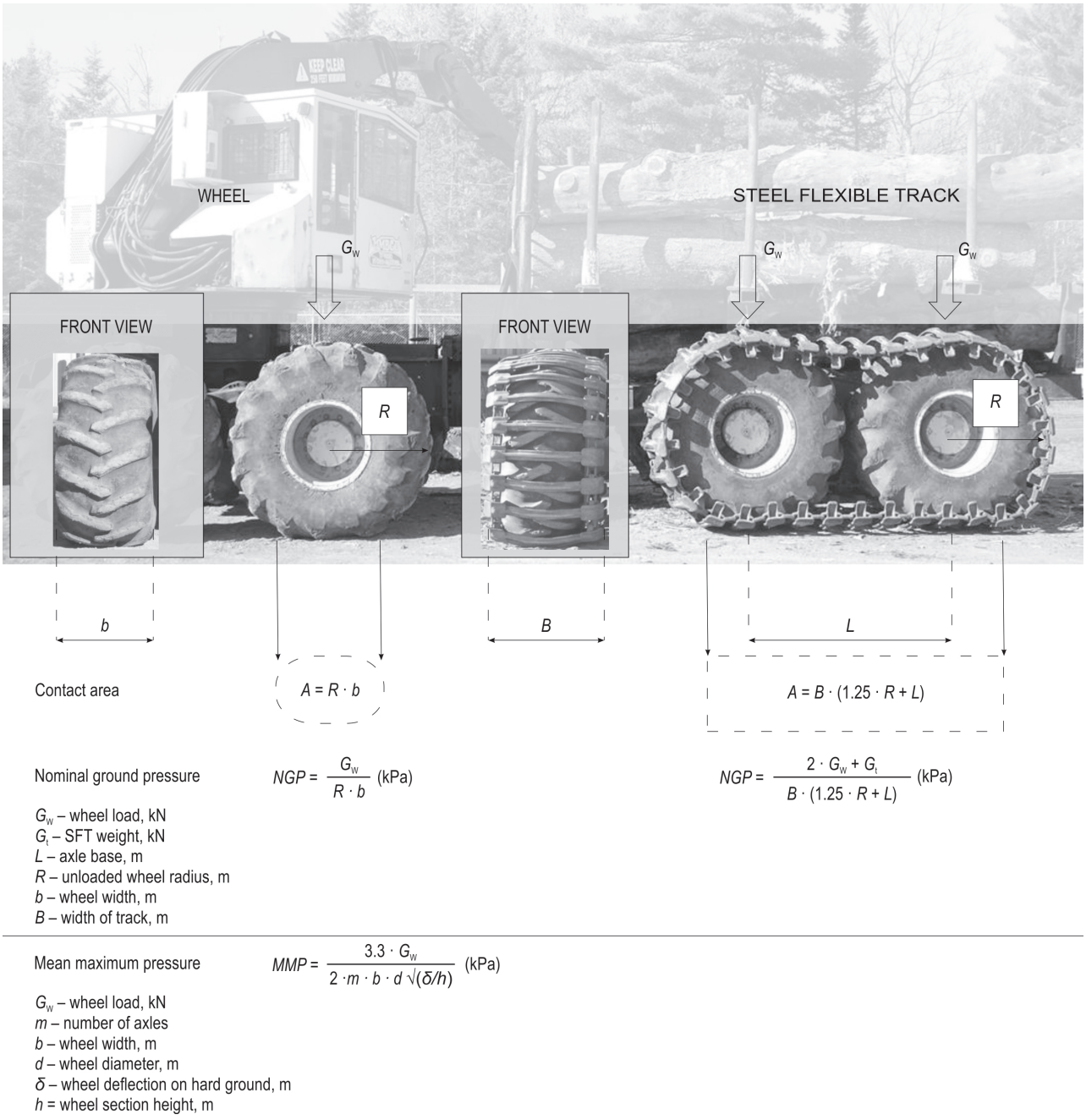

Fig. 12 Picture of Timbco TF820-D used for illustrating nominal ground pressure and mean maximum pressure formulae (NGP formulae from Mellgren (1980) and MMP formula from Rowland(1972)

⇒ the addition of SFT to an articulated machine made the forwarder more difficult to manoeuver and required more frequent steering corrections to maintain its position over the load test area.

When operated directly over steel, mean peak loads recorded underneath the front axle decreased by 11% between Scenario 1 and 2. With the addition of SFT on the rear bogie (combined mass of 2200 kg), no reduction of mean peak loads was expected under the front axle, but rather a potential increase. Due to the weight distribution between axles, loading the logbunk of a forwarder typically increases weight on the front axle by 8% compared to when unloaded (Makonnen 2007). Considering the mass of the added SFT (2200 kg) and the average increase of 8% to the front

axle, an additional 176 kg would have been distributed to the front axle, which should have contributed to slightly higher peak loads compared to when the forwarder was driven over the steel load test area without SFT. However, shearing of the front and rear axles over the load test area due to the articulation of the forwarder, likely caused a different load distribution pattern in relation to loading plates thereby influencing the magnitude of peak loads.

4.3 Wheels versus tracks on sand

Creating a flexible surface, upon which SFT and wheels could operate, was important to emulate application conditions in the forest by increasing contact area between the running gear and testing surface as opposed to when the running gear was operated directly over the steel load test area. The addition of a sand layer in itself lowered peak loads and surface contact pressures by placing further vertical distance between the load and the recording devices. Average peak load reduction underneath the front unloaded axle due to the presence of the 20 cm sand layer was calculated to be 11%. Based on Boussinesq's (1885) equation for stress propagation, Steinbrenner (1936) developed influence coefficients (I_3) for calculating the vertical stress distribution in soils caused by a rectangular loaded area using the load per unit area (q) and the vertical stress increase ($\Delta\sigma_z$) resulting at a certain depth (z) from a loaded area of length (L) and width (B) is obtained by applying Eq. 2:

$$\Delta\sigma_z = qI_3 \qquad (2)$$

where:

$$I_3 = \frac{2}{\pi}\left[\frac{m_1 n_1}{\sqrt{1+m_1^2+n_1^2}}\frac{1+m_1^2+2n_1^2}{\left(1+n_1^2\right)\left(m_1^2+n_1^2\right)} + \sin^{-1}\frac{m_1}{\sqrt{m_1^2+n_1^2}\sqrt{1+n_1^2}}\right]$$

$$m_1 = \frac{L}{B} \qquad n_1 = \frac{z}{b} \qquad b = \frac{B}{2}$$

Based on Eq. 2 and a loaded area of 0.195 m^2 (L= 0.273 m, B= 0.714 m), the 20 cm layer of sand (z=0.20 m) added on top of the steel platform lowered applied loads at the bottom by 34% compared to loads recorded directly under the wheel (Fang and Daniels 2006). The loaded area described above relates to the contact area below a 28L-26 Firestone tire as equipped on the forwarder, assuming a 7.6 cm penetration within the sand layer. There is a factor of three between results from the stress distribution formula (34%) and the measured reduction incurred by the sand layer at the load test area (11%). The stress propagation theorem is based on elastic theory and only provides an approximation since it was derived for homogeneous, isotropic materials of semi-infinite extent. Steinbrenner's influence coefficients also assume uniform load distribution below the loaded area and the pressure determined from the influence coefficient is directly below the center of the loaded area (Liu and Evett 1992). The sand used in Scenario 3 was located on top of a rigid surface, thus not having the same properties in all directions. Moreover, unlike the assumptions made with stress propagation theorem, load distribution below a forwarder wheel is not uniform, especially when operated over a rigid surface. As the forwarder was driven over the sand covered load test area, sand was compacted and the running gear sank into the sand further with increasing passes, thereby reducing the vertical distance between the contact area and steel loading plates. A reduction of this vertical distance (z) would yield a higher influence coefficient, which in turn would lower stress propagation. These conditions likely influenced the percent reduction described above. For example, using the same values as described above (L=0.273 m, B= 0.714 m), but for a vertical distance of 0.10 m, would yield a reduction of 10% instead of 34% when using a vertical distance of 0.20 m. There is an interaction between the sand-wheel/track interface and the physical properties of the sand, which enables it to distribute loads laterally.

Operating the forwarder on a flexible surface produced the lowest mean peak loads of all three scenarios, for both wheels and SFT. The sand layer allowed sinkage of the wheel or SFT/wheel combination, thus permitting an increased contact area to distribute applied loadings. Considering the influence of the sand layer on stress distribution, we calculated that SFT reduced mean peak loads by about 30% compared to wheels. This percent reduction is much less than the 54% reduction obtained using the NGP method or the 50% reported by Olofsfors (2009). However, unlike previous studies, dynamic loads and surface contact pressures were presented in this study and a 30% reduction of mean peak load remains significant. When operated on sand, only 19% of mean peak pressures recorded below the loaded rear wheels equipped with SFT exceeded the DSCPT of 150 kPa compared to 100% for the front wheels, indicating clear advantages of using SFT for protecting the physical environment during off-road traffic.

4.4 Accuracy of load test platform

The design of the load test platform proved to be useful and adequate to allow dynamic testing of full-

scale forest equipment. Peak pressures discussed in this article assume uniform pressure over a loading plate. In reality, once a wheel was located over a virtual active area, a variation of pressure was created over this area with a local peak. This effect is somewhat balanced or mitigated to some degree by the sharing of most wheel loads across multiple load cells. Despite having the option to technically accommodate 84 load cells, the load test platform was only equipped with 24 due to budgetary constraints. A higher number of load cells would not have increased the resolution but would have allowed a larger area of the platform to be monitored. In further studies, it is also recommended to install strain gauges below the steel loading plates to obtain more detailed information and complement the load data measured by the load cells. By measuring the micro deflections of the steel loading plates, more detailed information on stress propagation could be obtained.

Axle load comparisons between static results from the platform and those from portable scales showed an axle load overestimation of 6.1% at the platform. Portable scales used for cross-reference were designed for load control of vehicles used in road transportation. These vehicles are usually equipped with much narrower wheels than those installed on the tested forwarder. To circumvent this limitation, two portable scales were positioned alongside one another so as to form a wider scale and linked with a connecting cable. Once connected together, the load output was automatically calculated as the sum of the two scales. With this scale configuration, it is possible that a portion of the wheel load was not captured, thus potentially underestimating the true axle load. From these cross-reference tests, results from the load test platform seem to slightly overestimate loads recorded at the cluster level compared to the other two measuring systems.

5. Conclusions

Minimizing soil disturbances during mechanized forest operations, in particular heavy loadings beyond soil bearing capacity, is advantageous towards maintaining machine trafficability, site integrity including soil and water quality, and tree growth. Nominal ground pressure, commonly used as a criterion to predict the effect of a machine's weight and running gear characteristics on soil physical properties, can significantly underestimate the true impact on soils, particularly on harder soils that do not permit deep tire tread or track penetration. Dynamic forces and actual load distribution underneath a wheel or SFT greatly increase peak loads exerted below forest machines. Avoiding high peak loads is crucial in mitigating the effect of heavy machines on forest soils.

Since conventional weighing systems were not appropriate to address the specific testing requirements, a prototype system for measuring actual load distribution below wheels of forest machinery was designed and evaluated. Once constructed, the load test platform allowed to quantify the effects of SFT on forwarder load distribution.

Despite having the main purpose of increasing machine traction, SFT operated on the sand covered load test area did lower dynamic peak loads on average by 30% (considering the load distributing effect of the added sand layer) compared to loads exerted below wheels operated on sand. To our knowledge this was the first time dynamic load distribution below SFT was assessed. The operation of a forwarder equipped with SFT should greatly reduce peak pressures exerted on the operating surface, thereby helping to maintain soil health and plant productivity, in particular if the soil permits the full contact of the SFT/wheel surface.

Acknowledgements

Financial assistance was provided by the Natural Sciences and Engineering Research Council of Canada, FPInnovations, the University of New Brunswick, the New Brunswick Department of Transportation, and Debly Forest Services Limited. The authors are grateful for manuscript revisions provided by Dr. Robert J. Rogers from the Mechanical Engineering Department at the University of New Brunswick and Mr. Mark Partington from FPInnovations. We also acknowledge the assistance of Dr. Robert J. Rogers in designing the prototype load test platform. Technical assistance provided by Mr. Michael Downing, Mr. Marcel Labelle, Mr. Benjamin J. Poltorak, and Mr. Scott Fairbairn was appreciated. Statistical consultations were generously provided by Dr. William Knight from the Mathematics Department at the University of New Brunswick.

6. References

ASTM D 698, 2000: Test method for laboratory compaction characteristics of soil using standard effort (12,400 ft-lbf/ft^3; 600 kN-m/m^3). Am Soc Test Mater: 69–76.

ASTM D 422–63, 2002: Standard test method for particle-size analysis of soils. Am Soc Test Mater: 10–17.

ASTM A36/A36M, 2004: Standard specifications for carbon structural steel. Am Soc Test Mater: 108–110.

ASTM D 2487, 2011: Standard practice for classification of soils for engineering purposes (Unified Soil Classification System). Am Soc Test Mater, 12 p.

Batelaan, J., 1998: Development of an all-terrain vehicle suspension with an efficient, oval track. J Terramechanics 35(4): 209–223.

Boussinesq, J., 1885: Application des potentiels à l'étude de l'équilibre et du mouvement des solides élastiques. Gauthier-Villais, Paris, France, 721 p.

Brais, S., 2001: Persistence of soil compaction and effects on seedling growth in Northwestern Quebec. Soil Sci. Soc. Am. J. 65(4): 1263–1271.

Bowles, J.E., 1992: Engineering properties of soils and their measurement, fourth edition. Irwin McGraw-Hill, New York, NY, USA; ISBN: 0071129219, 241 p.

Bygden, G., Eliasson, L., Wästerlund, I., 2004: Rut depth, soil compaction and rolling resistance when using tracks. J. Terramechanics 40(3): 179–190.

Bygden, G., Wästerlund, I., 2007: Rutting and soil disturbance minimized by planning and using bogie tracks. Forestry studies 46(1): 5–12.

Clark Forest Machine, 2004: Tracks Handbook. http://www.arbrobec.ca/pdf/clark.pdf [Accessed on April 7, 2010]

Edlund, J., Bergsten, U., Arvidsson, H., 2013: A forest machine bogie with bearing capacity dependent contact area: acceleration and angular orientation when passing obstacles and drawbar pull force and free rolling resistance on firm ground. Silva Fennica 47(3): 7 p.

Eliasson, L., Wästerlund, I., 2007: Effects of slash reinforcement of strip roads on rutting and soil compaction on a moist fine-grained soil. For. Ecol. Manage. 252(1): 118–123.

Fang, H.-Y., Daniels, J.L., 2006: Introductory Geotechnical Engineering. An Environmental Perspective. Spon text. Taylor and Francis, London, UK, ISBN: 10: 0–415–30401–6, 545 p.

Frey, B., Kremer, J., Rudt, A., Sciacca, S., Matthies, D., Luscher, P., 2009: Compaction of forest soils with heavy logging machinery affects soil bacterial community structure. European Journal of Soil Biology 45(4): 312–320.

Froehlich, H.A., Miles, D.W.R., Robins, R.W., 1986: Growth of young *Pinus ponderosa* and *Pinus concorta* on compacted soils in Central Washington. For. Ecol. Manage. 15(4): 285–294.

Garber, M., Wong, J.Y., 1981: Prediction of ground pressure distribution under tracked vehicles I. An analytical method for predicting ground pressure distribution. J. Terramechanics 18(1): 1–23.

Gerasimov, J., Katarov, V., 2010: Effect of bogie track and slash reinforcement on sinkage and soil compaction in soft terrains. Croat. J. For. Eng. 31(1): 35–48.

Grecenko, A., 1995: Tyre footprint area on hard ground computed from catalogue value. J. Terramechanics 32(6): 325–333.

Han, H.-S., Page-Dumroese, D., Han, S.-K., Tirocke, J., 2006: Effects of slash, machine passes, and soil moisture on penetration resistance in a cut-to-length harvesting. Int. J. Forest Engineering 17(2): 11–24.

Hornback, P., 1998: The wheel versus track dilemma. ARMOR magazine March/April. 26 p.

International Road Dynamics, 2009: SAW Series 1 Portable scales. http://www.irdinc.com/privacy.php [Accessed on April 3, 2009.]

Jakobsen, B.F., Dexter, A.R., 1989: Prediction of soil compaction under pneumatic tyres. J. Terramechanics 26(2): 107–119.

Jansson, K.-J., Johansson, J., 1998: Soil changes after traffic with a tracked and a wheeled forest machine: a case study on a silt loam in Sweden. Forestry 71(1): 57–66.

John Deere, 2010: 1710 forwarder brochure. http://www.deere.com/en_US/cfd/forestry/deere_forestry/ forwarders/1710d_ general.html [Accessed on April 7, 2010]

Kleibl, M., Kvlač, R., Lombardini, C., Porhaly, J., Spinelli, R., 2014: Soil compaction and recovery after mechanised final felling of Italian coastal pine plantations. Croatian Journal of Forest Eng. 35 (1): 63–71.

Komandi, G., 1990: Establishment of soil-mechanical parameters which determine traction on deforming soil. J. Terramechanics 27(2): 115–124.

Kozlowski, T.T., 1999: Soil compaction and growth of woody plants. Scandinavian J. For. Res. 14(6): 596–619.

Labelle, E.R., Jaeger, D., 2012: Quantifying the use of brush mats in reducing forwarder peak loads and surface contact pressures. Croat. J. For. Eng. 33(2): 249–274.

Labelle, E.R., Jaeger, D., Poltorak, B.J., 2015: Assessing the ability of hardwood and softwood brush mats to distribute applied loads. Croat. J. For. Eng. 36(2): 227–242.

Liu, Cheng., Evett, J.B., 1992: Soils and Foundations. Third edition. Prentice Hall, Englewood Cliffs, NJ, USA, ISBN: 0138161828, 140–149.

Magagnotti, N., Spinelli, R., Güldner, O., Erler, J., 2012: Site impact after motor-manual and mechanised thinning in Mediterranean pine plantations. Biosystems Engineering 113(2): 140–147.

Makkonen, I., 2007: PASCAL ground pressure spreadsheet. FPInnovations, Pointe-Claire, QC. www.feric.ca/pascal-en.

McDonald, T.P., Seixas, F., 1997: Effect of slash on forwarder soil compaction. Int. J. Forest Engineering 8(2): 15–26.

McMahon, S., Evanson, T., 1994: The effect of slash cover in reducing soil compaction resulting from vehicle passage. LIRO report Rotorua, NZ. 19(1): 1–8.

Mellgren, P., 1980: Terrain classification for Canadian forestry. Canadian Pulp and Paper Association. Montreal, QC, Canada, 13 p.

Minitab Inc., 2010: Meet Minitab 16. http://www.minitab.com/uploadedFiles/ Shared_Resources/Documents/MeetMinitab/EN16_MeetMinitab.pdf, 122 p.

Murphy, G., Firth, J.G., Skinner, M.F., 2004: Long-term impacts of forest harvesting related soil disturbance on log product yield and economic potential in a New Zealand forest. Silva Fennica 38(3): 279–289.

Okamoto, I., 1998: How bogies work. Japan Railway & Transport Review 18: 52–61.

Olofsfors, 2009: Olofsfors bogie track manual. Olofsfors, Sweden, 20 p.

Olsen, H.J., Wästerlund, I., 1989: Terrain and vehicle research with reference to forestry at the Swedish university of agriculture. The Swedish university of agricultural sciences.

Department of operational efficiency. Garpenberg. No. 149, 60 p.

Owende, P.M.O., Lyons, J., Haarlaa, R., Peltola, A., Spinelli, R., Molano, J., Ward, S.M., 2002: Operations protocol for eco-efficient wood harvesting on sensitive sites. Project ECOWOOD, 74 p.

Partington, M., Ryans, M., 2010: Understanding the nominal ground pressure of forestry equipment. FPInnovations 12(5): 1–8.

Plamondon, J.A., 2006: Optimizing the results of harvesting with the protection of regeneration and of soils (HPRS): Best Practices Guide. FERIC Adv. Rep. 7(6): 6 p.

Poltorak, B.J., Labelle, E.R., Jaeger, D., 2018: Soil displacement during ground-based mechanized forest operations using mixed-wood brush mats. Soil and Tillage Res. 170: 96–104.

Poršinsky, T., 2005: Efficiency of Timberjack 1710B forwarder on roundwood extraction from Croatian Lowland forests. Dissertation. Faculty of Forestry University of Zagreb, 170 p.

Poršinsky, T., Stankić I., 2006: Efficiency of Timberjack 1710B forwarder on roundwood extraction from Croatian Lowland forests. Glasnik za šumske pokuse, special issue 5: 573–587.

Potau, X., Comellas, M., Nogués, M., Roca, J., 2011: Comparison of different bogie configurations for a vehicle operating in rough terrain. J. Terramechanics 48(1): 75–84.

Rowland, D,. 1972: Tracked vehicle ground pressure and its effect on soft ground performance. Proc. of the 4th conference of the Int. Soc. For Terrain-vehicle systems. Vol. 1. Stockholm, Sweden, 353–834.

Sakai, H., Nordfjell, T., Suadicani, K., Talbot, B., Bøllehuus, E., 2008: Soil compaction on forest soils from different kinds of tires and tracks and possibility of accurate estimate. Croat. J. For. Eng. 29(1): 15–27.

Silversides, C.R., Sundberg, U., 1989: Operational efficiency in forestry. Vol. 2. Practice. Kluver Academic Publishers, Dortrecht/Boston/London. 169 p.

SPSS, 2007: SPSS Base 16.0 User's guide. Chicago, IL, USA, 551 p.

Steinbrenner, W., 1936: A rational method for the determination of the vertical normal stresses under foundations. Proc. Int. Conf. Soil. Mech. Found. Eng. Cambridge Massachusetts. Vol. 2., 142–143.

Suvinen, A., 2006: Economic comparison of the use of tyres, wheel chains and bogie tracks for timber extraction. Croat. J. For. Eng. 27(2): 81–102.

TimberPro, 2002: Timbco TF-820-D forwarder specifications. http://timberpro.com/Modules/Old%20Brochures/820-D.pdf [Accessed on March 20, 2010]

Wong, L.Y., 2009: Terramechanics and off-road vehicle engineering. Second Edition. Butterworth-Heinemann. Amsterdam, 488 p.

Wronski, E.B., Humphreys, N., 1994: A method for evaluating the cumulative impact of ground-based logging systems on soils. Int. J. of For. Eng. 5(4): 9–20.

Authors' addresses:

Assist. Prof. Eric R. Labelle, PhD *
e-mail: eric.labelle@tum.de
Department of Ecology and Ecosystem Management
Technical University of Munich
Hans-Carl-von-Carlowitz-Platz 2
85354 Freising
GERMANY

Prof. Dirk Jaeger, PhD
e-mail: dirk.jaeger@uni-goettingen.de
Department of Forest Work Science and Engineering
Georg-August-Universität Göttingen
Büsgenweg 4
37077 Göttingen
GERMANY

* Corresponding author

Received: December 19, 2017
Accepted: March 19, 2018